

STIS/*HST* Observations of Large Magellanic Cloud Planetary Nebulae: A True Step Toward the Understanding of Planetary Nebula Morphology and Evolution

*L. Stanghellini (STScI/ESA), R. A. Shaw (STScI), M. Mutchler (STScI),
J. C. Blades (STScI), & B. Balick (UoW)*

The STIS/*HST* Survey of LMC PNs

Planetary Nebulae (PNs) have for many years been used as probes of the late stages of stellar evolution. While in many ways such studies have been very successful, and have inspired elaborate theoretical work on stellar evolution, they have been hampered by the great difficulty of determining accurate distances to PNs. As well, extinction within the Galaxy introduces substantial selection effects in the observed samples, making a direct comparison with theory very challenging. These are the single greatest limitations to further advances in the study of post-AGB evolution. These problems can now be addressed using the superior resolution and instrumentation of *Hubble Space Telescope*.

We have obtained images and slit-less spectra in a survey of Large Magellanic Cloud (LMC) planetary nebulae (*HST* Program 8271). These data on 27 targets were obtained with the Space Telescope Imaging Spectrograph (STIS). The data permit us to determine the nebular dimensions and morphology in the monochromatic light of several emission lines, including those that have traditionally been used for morphological studies in the Galaxy (H α , [N II] 6584 Å and [O III] 5007 Å), plus others of varying ionization, such as [O I], He I, and [S II]. The broad-band images allow us to determine the central star magnitudes (for the brighter stars), which yield the evolutionary state of the central stars. This paper examines the evolution of the nebulae themselves, with emphasis on the surface brightness evolution. We also present a preview of our work on the correlations between nebulae and stars. The images of Fig. 3 have been published by Shaw et al. (2001), while a comparison between the nebular abundances and morphology has been presented by Stanghellini et al. (2000). Our LMC sample is ideal for studying the co-evolution of PNs and their central stars, in that the debilitating uncertainties of the Galactic PN distance scale and the selection effects of interstellar dust do not apply, and the nebular dynamical ages can be used with greater confidence.

Morphology and Nebular Evolution

We classified the morphologies in our sample from the [O III] 5007 Å images (although we were guided by the [N II] 6584 Å images), using the classification scheme of Manchado et al. (1996). With this dataset, together with the ~30 LMC PNs for which monochromatic images exist in the *HST* archive (see Stanghellini et al. 1999), we can for the first time explore the question of temporal evolution of the nebular morphology by examining the change in surface brightness of nebulae as a function of nebular size (Fig. 1). Only two nebulae are spatially unresolved (one of those is probably a symbiotic star), and the rest are larger than 0.36 arcsec (~7 pixels) in diameter. This is probably a result of discovery selection, in that the presence of the [O III] lines is often a prerequisite for classification as a PN.

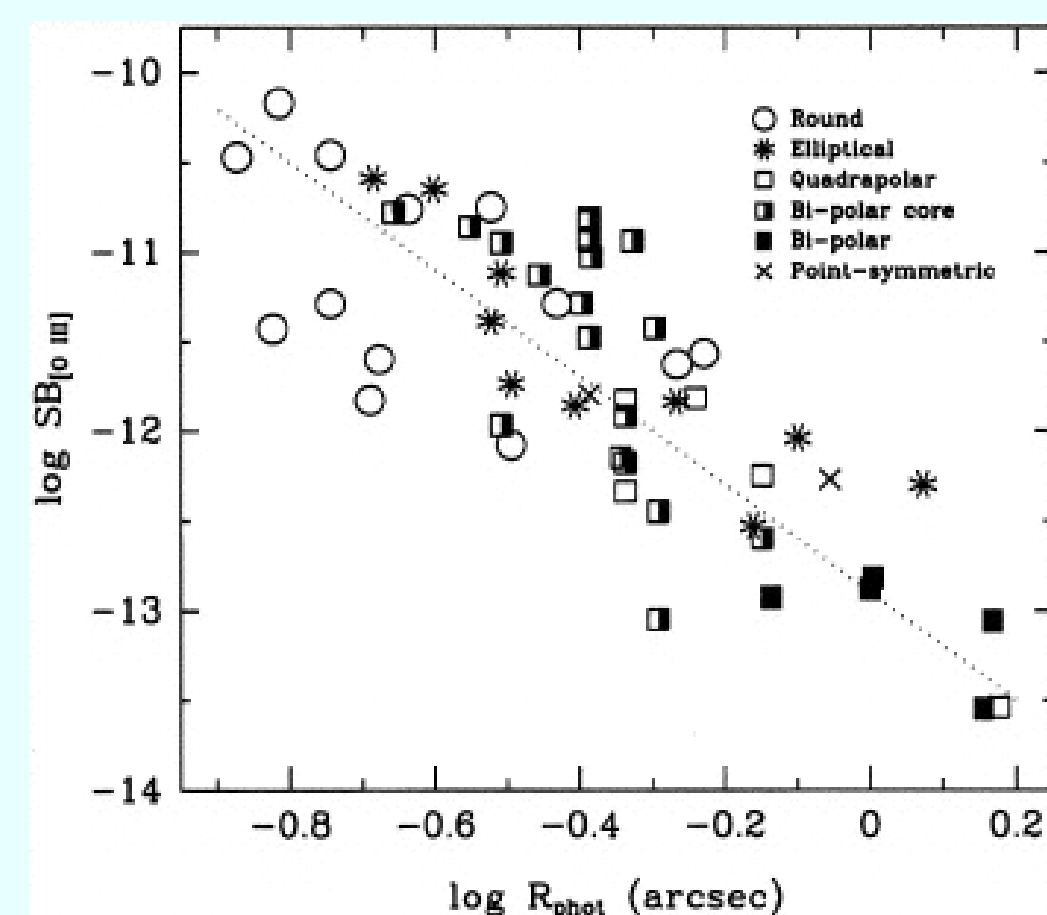


Figure 1: The decline of surface brightness (in the light of [O III] 5007 Å) with nebular radius consistent with $SB \sim R_{\text{phot}}^{-3}$ (dotted line). The segregation of some morphological types is likely a result of real evolution of morphological type, although classification ambiguity at small radii cannot be ruled out (see text). Two nebulae in this sample (not shown) are unresolved.

Figure 1 shows that most of the angularly smallest nebulae ($0''.17 < R < 0''.28$) are round or elliptical. In this size regime the nebulae are well resolved (>11 pixels diameter), so the lack of asymmetric nebulae here could indicate an evolutionary effect, in the sense that any initial asymmetry in the gas distribution and velocity field may not have had time to manifest itself in the morphology. Note, however, that the onset of asymmetric features appears even in very young nebulae (< 2000 yr), suggesting that the gross features of the nebular morphology are well connected to PN formation. As well, the possibility of ambiguity in our morphological classification, the small number statistics in this ([O III]-selected) sample, and possible selection effects, makes firm conclusions about evolutionary effects in young PNs difficult. What is more clear is the segregation of bi-polar core PNs (between $0''.30 < R < 0''.60$), which have a round or elliptical outer contour, and pure bi-polar nebulae ($> 0''.60$, or ~0.15 pc). This suggests that the bi-polarity may become the dominant morphological feature during the lifetime (after ~5000 yr) of bi-polar core nebulae, perhaps through subsequent shaping by the radiation field and wind from the central star (Balick 1987). Our data also show that the incidence of non-symmetric nebulae (including bi-polar nebulae, which is an indicator of Population I ancestry in the Galaxy) is much higher than that reported for the Galaxy. This result, although intriguing, could also be a consequence of the selection effect that underestimates the number of asymmetric PNs in the Galactic plane, due to interstellar extinction.

Nebular Evolution and the Ionization Structure

Let us examine the surface brightness decline for all PNs in our STIS/*HST* survey observed to date, by inspecting the various *monochromatic* images. In Fig. 2 we plot SB against R_{phot} for most of the recombination and forbidden line images. A simple relation between nebular mass and radius exists, that can be used to infer the nebular mass, if the radius is known. In fact, the Emission Measure can be expressed as $EM \sim M_{\text{PN}}^2/V$, where M_{PN} is the nebular mass, and V the nebular volume; thus, the surface brightness can be expressed as $SB \sim M_{\text{PN}} R^{-5}$. Using our observational findings of Figs. 1 and 2, we infer that $M_{\text{PN}} \sim R_{\text{PN}}$. This very simple relation allow us to infer, from Fig. 1, that asymmetric PNs have, on average, larger nebular mass. It seems only natural that these high mass PNs would derive from the higher mass stars.

The relations above hold only in the cases in which the nebular density (N_e) is smaller than the critical density (N_{crit} , the density at which the collisional de-excitation rate balances the radiative transition rate). We have measured the critical density for the ions considered in Figs. 1 and 2, and we found that $N_e < N_{\text{crit}}$ for all the PNs examined.

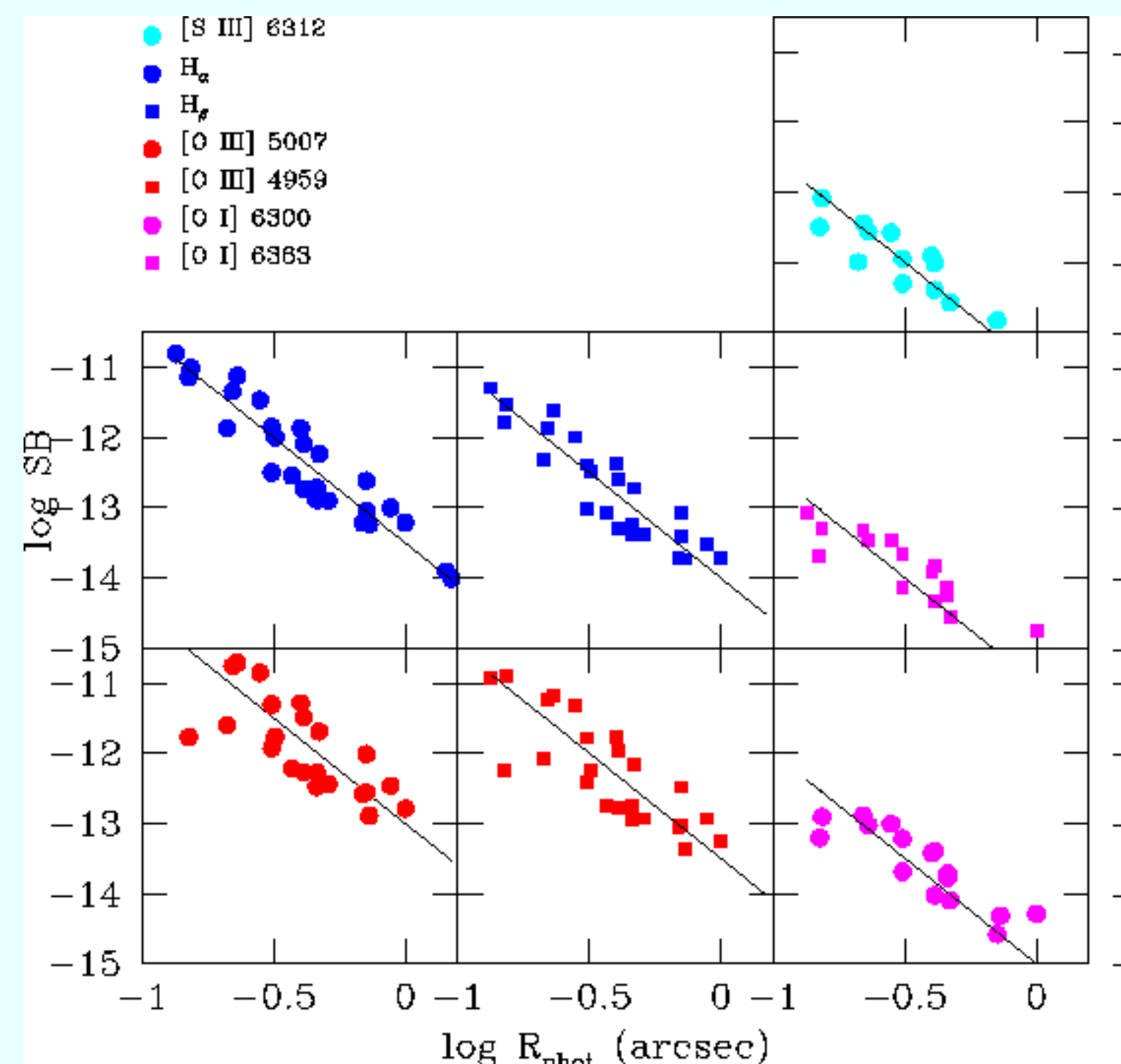


Figure 2: Surface brightness decline for the multiwavelength images of the PNs in our STIS survey. The solid lines represent the surface brightness decline as in Fig. 1, $SB \sim R_{\text{phot}}^{-3}$. The photometric radii are measured from the [O III] 5007 Å images.

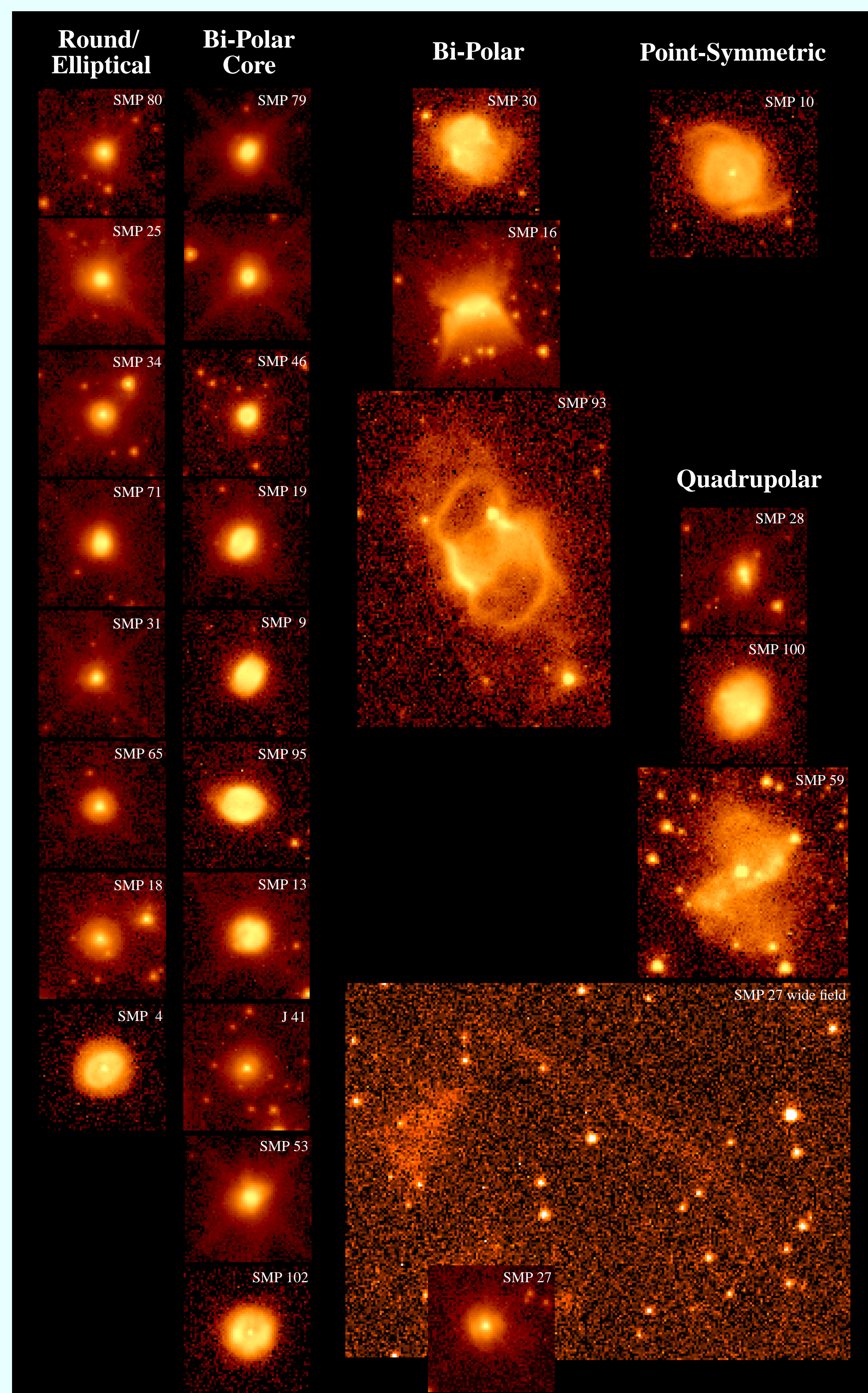


Figure 3: Broad-band, false-color images of each of the observed LMC nebulae in our STIS program, arranged by morphological type. All images are on the same spatial scale, with a square-root intensity stretch; the field of view in most images is 3 x 3 arcsec. The physical scale is ~0.245 pc/arcsec.

Let us now examine the cases in which the electron density of the PNs is higher than the critical density. In Fig. 4 (top panels) we plot the usual SB vs. R_{phot} relation, from the observations in the light of [S II]. The critical densities, calculated for a model nebula with $T_e \sim 10,000$ K and $N_e \sim 1000 \text{ cm}^{-3}$, are respectively $N_{\text{crit}} \sim 3.6 \times 10^3 \text{ cm}^{-3}$ for the 2->1 transition (6731 Å), and $1.4 \times 10^3 \text{ cm}^{-3}$ for the 3->1 transition (6717 Å). We have compared these critical densities with the electron density of the PNs, and plotted separately, in Fig. 4 (bottom panels) the PNs in which $N_e > N_{\text{crit}}$. From the top panels, we can infer that a simple $SB \sim R_{\text{phot}}^{-3}$ relation does not hold for the majority of the PNs at these wavelengths.

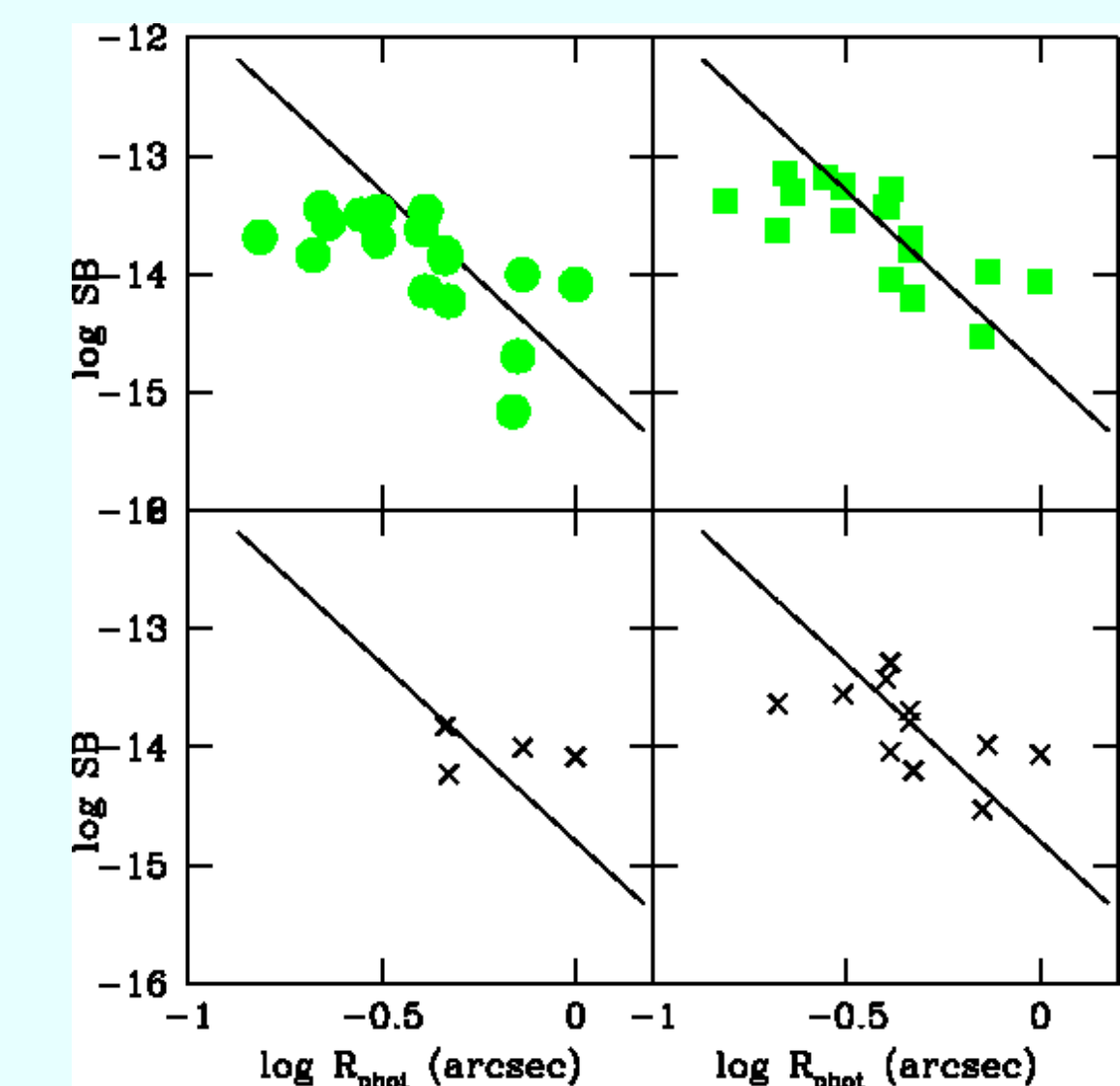


Figure 4: The SB vs. R_{phot} relation for the [S II] forbidden lines. Top panels: full sets of data for [S II] 6717 (top left) and [S II] 6731 (top right). Bottom panels: PNs with $N_e > N_{\text{crit}}$, for [S II] 6717 (bottom left) and [S II] 6731 (bottom right).

On the other hand, most nebulae are less dense than the critical density for the [S II] 6717 Å line, and a sizable fraction of them are less dense than the critical density for the 6731 Å line. This effect explains the different SB to R_{phot} relation observed.

Stellar and Nebular Evolution

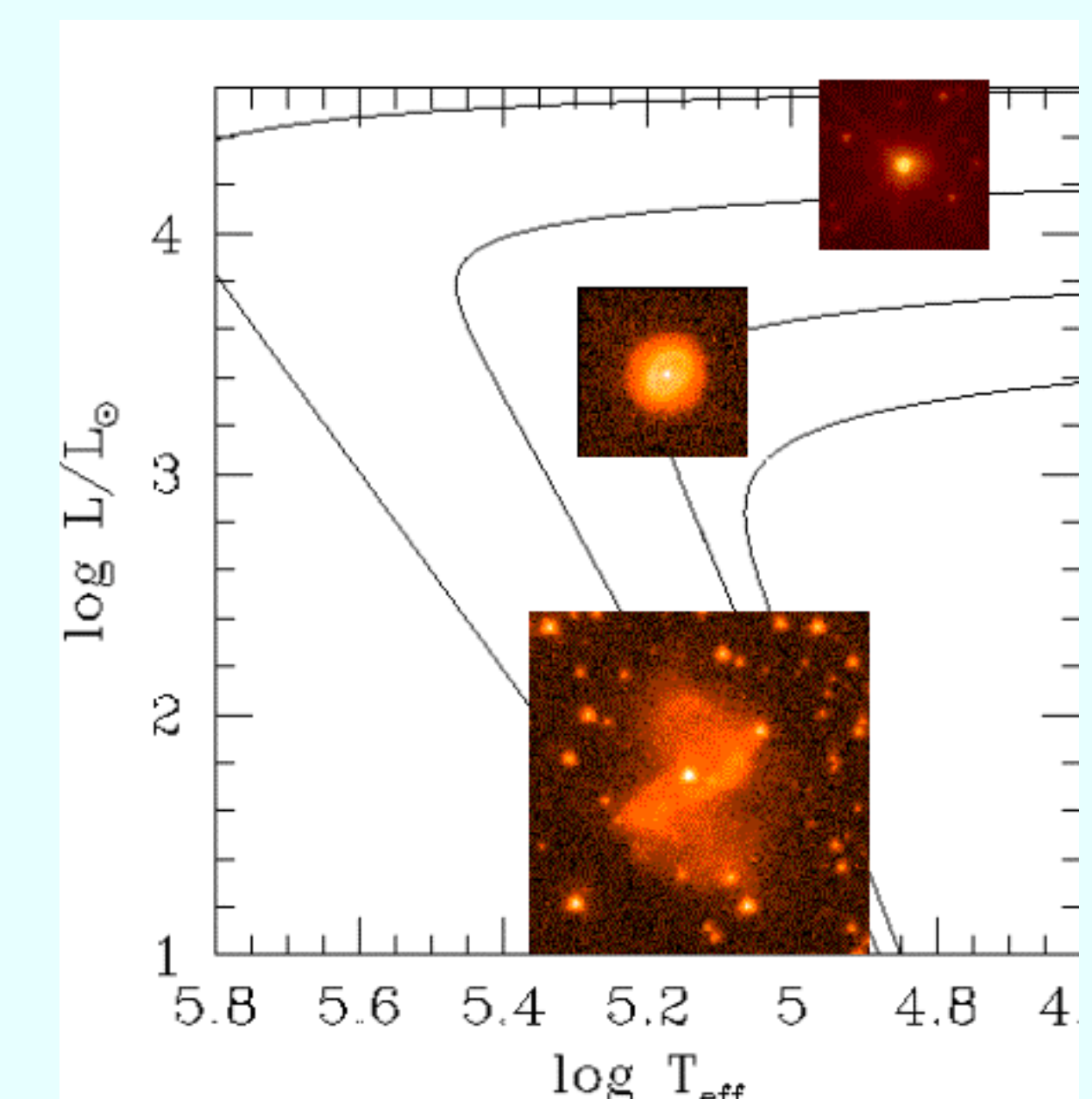


Figure 5: Three PN images located in the positions of their central stars on the HR diagram. Tracks correspond to central star masses of 0.55, 0.6, 0.8, and 1.2 solar masses.

A quick preview on the correlations between stellar and nebular evolution, as studied from our images, is offered in Fig. 5, where the central stars of three PNs in our sample have been located in the HR diagram. We use luminosities derived by stellar photometry, and stellar temperatures from the Zanstra analysis. It is worth mentioning that this plot is the first ever direct comparison between stellar evolution and nebular expansion for low and intermediate mass stars, since it is the first time that central stars of known distances have been directly observed. It is clear from Fig. 5 that the more evolved stars are hosted by the dynamically evolved nebulae. A great advantage of these studies is the direct estimate of the transition (post-AGB) time from the difference between the stellar evolutionary time, and the nebular expansion time.

Conclusions

This study of LMC PNs, which is still underway, has given us significant insight into the formation and evolution of the nebulae and their central stars. For the first time we can study a relatively unbiased sample of PNs to examine the formation and evolution of the nebulae. Specifically, there is good evidence for at least some evolution in the morphological type as PNs age. As well, this morphological study places some constraints on the mechanism for PN formation.

Studying the surface brightness decline versus the photometric radii is very effective in tracking the ionization structure of the nebulae, their plasma structure, and the density distribution. The data set from our LMC survey is ideal to constrain the nebular photoionization models, built for the understanding of these complicated objects.

Finally, this study will permit a much more detailed examination of predictions from stellar evolution theory, particularly when the analysis of the central stars is complete.

Acknowledgement: Support for this work was provided by NASA through grant GO-08271.01-97A from ST ScI.

References:

- Balick, B. 1987, *AJ*, 94, 671
- Manchado, A., Guerrero, M. A., Stanghellini, L. & Serra-Ricart, M. 1996, *The IAC Morphological Catalog of Northern Galactic Planetary Nebulae* (Tenerife: IAC)
- Shaw, R. A., Stanghellini, L., Mutchler, M., Balick, B., & Blades, J. C. 2000, *ApJ*, 548, 727
- Stanghellini, L., Blades, J. C., Osmer, S. J., Barlow, M. J. & Liu, X.-W. 1999, *ApJ*, 510, 687
- Stanghellini, L., Shaw, R. A., Balick, B., & Blades, J. C. 2000, *ApJ*, 534, L167